LOI12-18-001

A Letter of Intent to the Jefferson Lab PAC 46

Measurement of the parameters of the LHCb pentaquark states through double polarization asymmetries with SBS in Hall A

C. Fanelli

MIT, Cambridge, MA 02139

L. Pentchev, B. Wojtsekhowski

Thomas Jefferson National Accelerator Facility, Newport News, VA 23606

June 4, 2018

Contents

Abstract

We present this Letter-of-Intent to the Jefferson Lab Program Advisory Committee (PAC46) and plan to prepare a full proposal with the goal to do a high sensitivity search of the recently claimed pentaquarks and study their parameters: branching ratio to pJ/ψ, spin, parity, and t-dependence, in the s-channel photoproduction: $\gamma p \to P_c \to J/\psi(e^+e^-) + p'$. It will utilize the GEp/SBS detector system in Hall A to detect all three particles in the final state. Measuring the polarization observables A_{LL} and K_{LL} (with respect to the beam photon and target/recoil proton) will bring the study of the two pentaquarks, $P_c^+(4380)$ and $P_c^+(4450)$, to a much precise level as compared to the cross-section measurements. While the narrow $P_c^+(4450)$ state, if exists, can be seen as a peak in the energy dependence of J/ψ cross-ection, the wide $P_c^+(4380)$ resonance covering almost the whole JLab energy range can't be interpreted without polarization measurement. The proposed measurement will take advantage of the Super Bigbite setup developed for the GEp/SBS experiment in Hall A, which consists of an hadron arm (SBS) and an electron arm (ECAL). Experiment will use a circularly polarized photon beam and a longitudinally polarized target for the initial helicity state correlation A_{LL}, whereas for the polarization transfer K_{LL} a proton polarimeter of the GEp setup in the SBS arm.

This project is supported by the recent calculations developed in collaboration with JPAC: the polarization observables are dramatically sensitive to parameters of pentaquarks states and their determination would allow to get a comprehensive picture of these new P_c^+ states. Jefferson Lab beam allows to produce the LHCb pentaquarks near J/ψ threshold via photo-production which was already addressed in several approved proposals aiming to search for P_c^+ states by cross-section measurements. Our project is complementary to such proposals, and will provide additional information on P_c^+ but with much higher sensitivity. The A_{LL} and K_{LL} parts will constitute two independent measurements based on the same detector apparatus. High performance of the proposed experiment is defined by the selected detector apparatus and optimized geometry of experiment. Projected accuracy for each observable (A_{LL} and K_{LL}) is about 0.13 for the case of 2% branching of for the $P_c^+(4450)$ resonance decay for J/ψ+p and 20 days of data taking for each of the two measurements.

1 Introduction

Why studying the pentaquarks? The bound states of hadron matter are very useful for studing of the fundamental aspects of QCD. Although predicted by Gell-Mann [1] decades ago, pentaquarks turned to be unexpectedly difficult to discover. There is nothing in principle that prevents quarks from forming 'exotic' hadrons beyond ordinary mesons and baryons, for example aggregating four quarks and one antiquark to form a pentaquark. The study of these states allow to shed light on the fundamental properties of QCD, in particular on color confinement.

About fifteen years ago, several experiments claimed to observe pentaquark states. In particular, in 2003, the LEPS experiment [2] reported the observation of a narrow nK^+ peak (called Θ^+) at a mass of 1540 MeV/c^2, with a quoted significance of 4.6 standard deviations, and an even stronger signal was seen by ELSA on Fig. 1 (left). This result was followed by other experiments that claimed to observe a narrow peak at a mass close to 1540 MeV/c^2 in the channels nK^+ or pK^0. Further evidence in support of pentaquark states seemed to come from the claimed observations of a doubly-charged state $ssdd\bar{u}$ corresponding to 1862 MeV/c^2 [3], and a neutral $uudd\bar{c}$ state at 3099 MeV/c^2 [4]. Nevertheless, none of these states was confirmed, and further analyses with high-statistics led to reduced significance in the peak, e.g. the g10a experiment at CLAS [5] confirmed the null result of the Θ^+ state. At the same time, a very robust observation in hadron channel was recently reported [6].

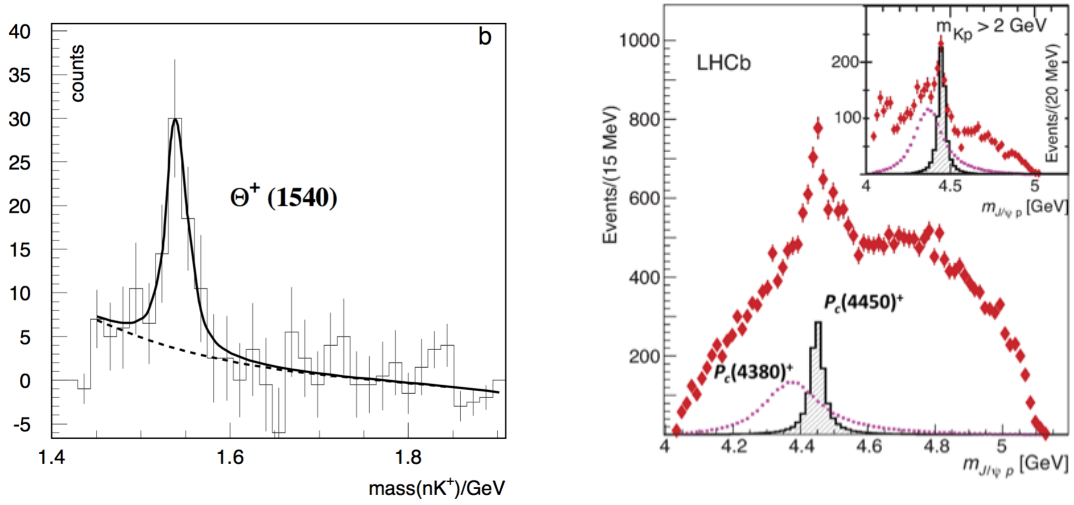

Figure 1: (left) The nK^+ mass distribution after side-bin subtraction of the background under the K^0_s at ELSA [7]. (right) The invariant mass of $J/\psi p$ from $\Lambda^0_b \to J/\psi p K^-$ decays, from LHCb [8].

A renewed interest in pentaquark searches followed after the recent results of the LHCb collaboration [8]: the clear peak seen in the $J/\psi\ +\ p$ spectrum (see Fig. 1 (right)) provided evidence for the existence of pentaquarks. Although the invariant mass projection exhibits a single peak structure, LHCb peak is consistent with the existence of two structures, $\mathrm{P}^+_\mathrm{c}(4380)$

and $P_c^+(4450)$, the first with mass of 4380 ± 40 MeV and width of 205 ± 100 MeV and second with the mass 4450 ± 4 MeV and width 38 ± 20 MeV. The LHCb data also suggests a preferred spin-parity assignment of $J^P = 3/2^-$ and $J^P = 5/2^+$ for the lighter and heavier states respectively. Nevertheless, the fit was not robust enough to exclude other combinations. These structures are believed to be resonances of hidden-charm pentaquarks, bound states with minimum constituent quark content of $uudc\bar{c}$ [9] but other interpretations as molecular bound states [10] or as a kinematic effect from proximity to other cross-channel thresholds are possible [11]. Many questions about these pentaquark states are open, including the t-dependence.

How do we measure the pentaquarks? The production of the LHCb pentaquark states from proton require a photon beam energy at least 10.1 GeV. Any experiment with sensitive search of the LHCb P_c^+ now would be useful, and there are already several ongoing experiments and proposals at JLab. GlueX in Hall D recently provided the first measurement of J/ψ at JLab [12] via photo-production on a proton target ($\gamma p \to J/\psi + p'$) using a tagged photon beam of about 10^7 γ/s above the J/ψ production threshold or the flux of 2.6×10^7 equivalent photon/s.

In a brief review of the J/ψ production experiments the most important parameter is the photon flux which we present in the units of equivalent photon per second, $N(\omega)$. An integral, $\int N(\omega) d\omega/\omega$, gives the photons flux in a given energy range. The second key parameter is an acceptance of the detector system. For the purpose of easy comparison the production rates were all adjusted to **the 2% branching ratio of the 4.45 GeV pentaquark decay to J/ψ+p**.

Hall B has proposed a measurement of the LHCb pentaquarks based on electro-production at very low Q^2 with CLAS12 [13] at an effective photon flux of 2.5×10^9 equivalent photon/s providing photon-proton luminosity 5×10^{32}. The resulting rate of the pentaquark related events is on the level of a 125 per day (in 50% detection acceptance reported in the proposal). About the same amount of events will be recorded using the untag mode.

The SoLID detector, proposed for construction in Hall A [14], is a large acceptance detector that will allow measuring of electro-production J/ψ in the process $ep \to e' J/\psi + p'$ at an effective photon flux of 4.5×10^{10} equivalent photon/s. The resulting rate of J/ψ+p events is of 42 per day. However, the designed experiment requires detection of the scattered electron with minimum energy of 1 GeV which precludes observation of the 4.45 GeV state.

Hall C proposed a measurement [15] of the J/ψ photo-production for study the pentaquark states as a bump in the production cross section (only J/ψ decay products, e^+e^- and $\mu^+\mu^-$, will be observed) and rely on a big difference in t-dependence between the s and t channels of the reaction. The experiment will be done with high electron beam current . The high photon flux of 7×10^{12} equivalent photon/s is very productive in spite of small solid angle of the spectrometers which leads to very small acceptance of 3×10^{-5}. The resulting rate of events is of 120 per day.

Key considerations of the current experiment. Our project is complementary to those already proposed at JLab, as we propose an innovative approach allowing the measurement

of two polarization observables A_{LL} and K_{LL}. Configurations of the previously proposed experiments do not allow A_{LL}/ K_{LL} double polarization measurements due to low projected statistics, lack of the proton polarimeter or high electron beam current which precludes use of the polarized target.

We suggest to take advantage of the GEp/SBS apparatus which two arms have 60 and 180 msr solid angles and includes a proton polarimeter. With two-body kinematics of the final state (J/ψ + p) and the two-body kinematics of the J/ψ decay to an electron-positron pair we find the possibility to arrange the geometry of a two-arm apparatus with high detection efficiency (0.65%) for events with all three particles - a proton, a positron, and an electron. The high momenta of the produced electron and positron allow a good suppression of the background already on a trigger level and the exclusivity of the reaction allows to reconstruct the proton track and momentum. With the photon flux of 2.6×10^{12} equivalent photon/s and the acceptance 0.65% the resulting rate of detected $J/\psi + p$ events is 4400 per day (in K_{LL} measurement). Overall the production rate of the fully reconstructed $J/\psi + p$ events is large enough to measure the polarization observables. The accuracy of this measurement also benefits from a relatively low proton momentum for which the polarimeter method provides large efficiency and analyzing power (see more in Sec. 4).

As it will be described in Sec. 2, the polarization observables have a large distinguishing power of the P_c^+ spin-parity states, and can provide new insight on both the photo-coupling and hadronic coupling of the pentaquarks due to their high sensitivity. In Sec. 3, we describe the experiment that will be performed in Hall A. The high accelerator current combined with the high acceptance of the Super Bigbite Spectrometer will allow to measure not only the cross-section but also polarization quantities that are of critical importance for understanding the reaction mechanism. Preliminary results of the simulations and the description of the data analysis can be found in Sec. 4. Projections and further details are described in Sec. 5, while final considerations are summarized in Sec. 6.

Collaboration buildup status. The current list of proponents is a short one which is typical for LOI stage. The idea to detect J/ψ in SBS was first presented to the PAC in 2007 [16] and was strongly supported in the report [17], (see in the PAC report on page 12). More recently, the conceptual ideas were presented at the meetings of SBS collaboration [18] . An advanced poster has been presented at the APS meeting in April 2018 [19]. The analysis benefits from our work with GlueX J/ψ data and the proton polarimeters. The collaboration for this experiment will be based on the SBS group which is behind the GEp/SBS experiment. We are already discussing the plan of the A_{LL} measurement with the members of the polarized target group at UVa. On the theory of A_{LL}, K_{LL} for $J/\psi + p$ case we are collaborating with the JPAC group.

2 Theoretical Studies

The use of photo-production is especially appealing as an independent test of the pentaquark state existence. Compared to the LHCb measurement, the photo-production allows a cleaner approach to the $J/\psi(e^+e^-)p$ spectrum by removing the final-state interactions possibly present in the Λ_b^0 decay channel.

We discuss the feasibility of measuring (i) the initial state helicity correlation between the polarized photon beam and the polarized target proton $\mathrm{A_{LL}}$, and (ii) the polarization transfer to the recoil proton $\mathrm{K_{LL}}$. The study of both the pentaquark photo and hadronic couplings is a *terra incognita*, and we will show that these quantities are very suitable observables due to their sensitivity to the resonance amplitudes. These polarization observables are defined as:

$$\mathrm{A(K)_{LL}} = \frac{1}{2}\left[\frac{\frac{d\sigma(\uparrow\uparrow)}{dt} - \frac{d\sigma(\uparrow\downarrow)}{dt}}{\frac{d\sigma(\uparrow\uparrow)}{dt} + \frac{d\sigma(\uparrow\downarrow)}{dt}} - \frac{\frac{d\sigma(\downarrow\uparrow)}{dt} - \frac{d\sigma(\downarrow\downarrow)}{dt}}{\frac{d\sigma(\downarrow\uparrow)}{dt} + \frac{d\sigma(\downarrow\downarrow)}{dt}}\right] \tag{1}$$

where in the case of $\mathrm{A_{LL}}$ the first arrow refers to the incident photon polarization whereas the second arrow refers to the direction of the proton polarization at target, and the axis is that of the beam for both arrows. The definition of $\mathrm{K_{LL}}$ is similar, but the second arrow now refers to the spin polarization of the recoil proton in the direction of the recoil proton momentum.

2.1 The JPAC Model

The processes contributing to $\gamma p \to P_c \to J/\psi + p'$ are represented in the diagram of Fig. 2. The model is described in Ref. [20].

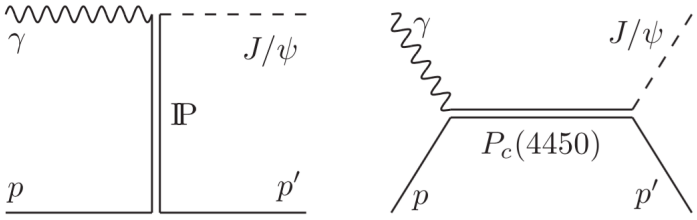

Figure 2: The dominant contributions to the J/ψ production, taken from [21]. (left) The non-resonant background is modeled by the exchange of a Pomeron; (right) the resonant contribution of the $\mathrm{P_c^+}(4450)$ is modeled by a Breit-Wigner.

The background is assumed to be dominated by diffractive photoproduction of the J/ψ off the proton target. In Regge theory, this is realized via pomeron exchange in the t-channel. An effective model, has been used where the kinematical factors are estimated as if the pomeron had vector quantum numbers [22]:

$$\langle \lambda_\psi \lambda_{\gamma'} |\, T_P \,| \lambda_p \lambda_\gamma \rangle = F(s,t)\, \bar{u}(p_f, \lambda_{p'}) \gamma_\mu u(p_i, \lambda_p) [\varepsilon^\mu(p_\gamma, \lambda_\gamma) q^\nu - \varepsilon^\nu(p_\gamma, \lambda_\gamma) q^\mu] \varepsilon^*_\nu(p_\psi, \lambda_\psi) \tag{2}$$

where $u(p_i, \lambda_p)$ and $u(p_f, \lambda_{p'})$ are the Dirac spinors of the initial and final protons respectively, q is the photon 4-momentum, and ε indicates the polarization vectors for the photon and J/ψ. The function $F(s,t)$ is a phenomenological function reproducing the energy dependence of the photo-production process to be fit to data.

The s-channel is assumed to be saturated by a single pentaquark resonance, which is parametrized with a simple Breit-Wigner form [21].

$$\langle \lambda_\psi \lambda_{p'} | \, T_r \, | \lambda_\gamma \lambda_p \rangle = \frac{\langle \lambda_\psi \lambda_{p'} | \, T_{\rm dec} \, | \lambda_r \rangle \, \langle \lambda_r | \, T^\dagger_{\rm em} \, | \lambda_\gamma \lambda_p \rangle}{M_r^2 - W^2 - {\rm i}\Gamma_r M_r} f_{\rm th}(s). \tag{3}$$

Here, M_r and Γ_r are the resonance mass and width, respectively, and $W = \sqrt{s}$ is the invariant mass. If the resonance decays in S-wave ($J^P = 3/2^-$), Eq. (3) will be finite at threshold. According to duality, the diffractive production should be roughly equal to the average of the resonant amplitude in the direct channel. The dominance of the signal over the background at threshold, far from the peak, looks thus unphysical, and an additional factor, $f_{\rm th}(s) = \left(\frac{s - s_t}{s} \frac{M_r^2}{M_r^2 - s_t} \right)^\beta$, has been added to suppress the resonance out of the peak, with $\beta = 1.5$.

Two amplitudes play an important role in (3): (i) the hadronic helicity amplitude $T_{\rm dec}$ and (ii) the electromagnetic decay: (i) The hadronic helicity amplitude $T_{\rm dec}$ describes the decay of the resonance of spin J to the $J/\psi\, p$ state takes the form

$$\langle \lambda_\psi \lambda_{p'} | \, T_{\rm dec} \, | \lambda_r \rangle = g_{\lambda_\psi \lambda_{p'}} d^J_{\lambda_r, \lambda_\psi - \lambda_{p'}}(\cos\theta), \tag{4}$$

where $g_{\lambda_\psi \lambda_{p'}}$ are the three independent helicity couplings between the resonance and the final state. Since currently no information about the behaviour of these couplings exists for the pentaquark, they are assumed to be of equal sizes, *i.e.* $g_{\lambda_\psi \lambda'_p} \equiv g$ for $\lambda_\psi - \lambda_{p'} > 0$ and $g_{\lambda_\psi \lambda'_p} \equiv \eta g$, where η is the naturality of the resonance. The helicity amplitudes and the partial decay width $\Gamma_{\psi p}$ are related by $\Gamma_{\psi p} = \mathcal{B}_{\psi p}\, \Gamma_r = \frac{\bar{p}_f}{8\pi M_r^2} \frac{6 g^2}{2 J_r + 1}$, with $\mathcal{B}_{\psi p}$ the branching ratio of $P_c \to J/\psi\, p$ and $\bar{p}_f$ the momentum p_f evaluated at the resonance peak. The $\mathrm{P}_\mathrm{c}^+(4450)$ decay is assumed to be dominated by the lowest partial wave according to the spin-parity assignment. (ii) The electromagnetic decay depends on two independent photocouplings, $A_{1/2}$ and $A_{3/2}$:

$$\langle \lambda_\gamma \lambda_p \, | T_{\rm em} | \, \lambda_R \rangle = \frac{W}{M_r} \sqrt{\frac{8 M_N M_r \bar{p}_i}{4\pi\alpha}} \sqrt{\frac{\bar{p}_i}{p_i}} A_{\lambda_R}, \tag{5}$$

with $\bar{p}_i$ the momentum p_i evaluated at the resonance peak. The electromagnetic decay width Γ_γ is then given by $\Gamma_\gamma = \frac{\bar{p}_i^2}{\pi} \frac{2 M_N}{(2J_r+1) M_r} \left[\left| A_{1/2} \right|^2 + \left| A_{3/2} \right|^2 \right]$. The photon helicity amplitudes for pentaquarks are estimated by means of the vector-meson dominance (VMD) model [23], assuming the following relation for the transverse vector-meson helicity amplitudes $\langle \lambda_\gamma \lambda_p | \, T_{\rm em} \, | \lambda_r \rangle = \frac{\sqrt{4\pi\alpha} f_\psi}{M_\psi} \langle \lambda_\psi = \lambda_\gamma, \lambda_p | \, T_{\rm dec} \, | \lambda_r \rangle$.

Here, f_ψ is the J/ψ decay constant, which has been estimated to be $f_\psi = 280$ MeV. Therefore, this VMD assumption leads to $\Gamma_\gamma = 4\pi\alpha\, \Gamma_{\psi p} \left(\frac{f_\psi}{M_\psi} \right)^2 \left(\frac{\bar{p}_i}{\bar{p}_f} \right)^{2\ell+1} \times \mathcal{P}_t$, where the

factor $\mathcal{P}_t$ takes into account that only the transverse polarizations of the J/ψ contribute. The initial assumption is then relaxed in order to study the behavior at different relative sizes of $A_{1/2}$ and $A_{3/2}$, keeping their quadrature sum $\sqrt{|A_{1/2}|^2 + |A_{3/2}|^2}$, and the size of the hadronic couplings g unchanged.

2.2 Prediction of the observables

Predictions for A_{LL} and K_{LL} (see Eq. (1)) based on the model described above can be found in the following plots. We assumed in every plot an hadronic branching ratio of 2% (for both the LHCb pentaquark states). The total photo-production cross section of a $P_c^+(4450)$ $5/2^+$ with 2% BR is shown in Fig. 3.

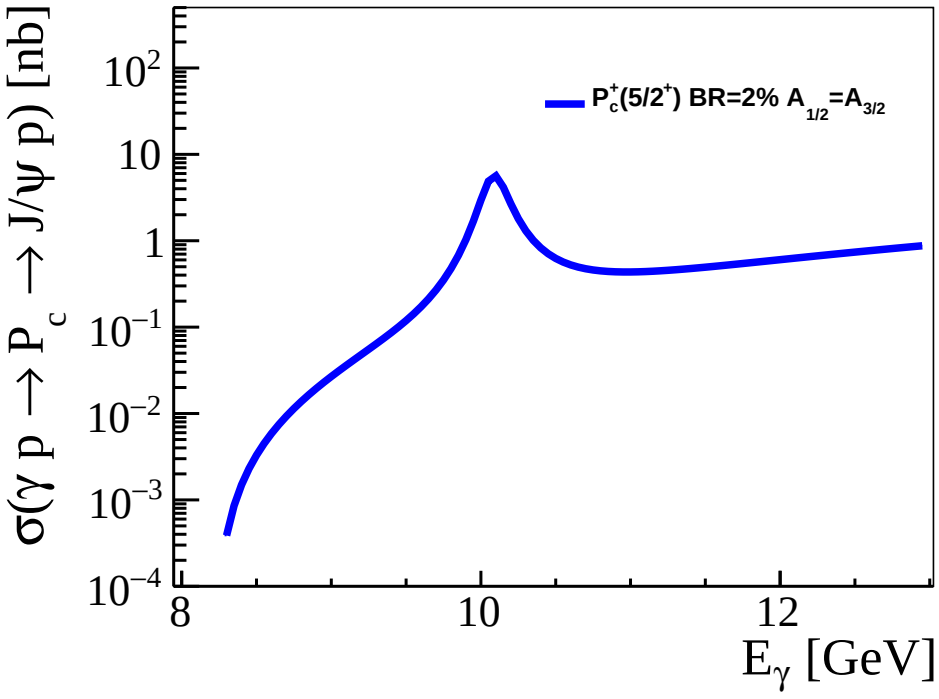

Figure 3: The photoproduction cross-section of the process $\gamma p \to P_c \to J/\psi + p'$ corresponding to $P_c^+(4450)$ $5/2^+$ with 2% hadronic BR. At the resonance energy the cross-section is about 5 nb.

This choice is arbitrary and motivated by comparison with other proposed experiments. When both the resonance contributions are shown, we assume the following spin-parity assignment: $P_c^+(4450)$ $5/2^+$ and $P_c^+(4380)$ $3/2^-$.

Fig. 4 shows the differential cross-section as a function of the scattering angle in the center of mass for the two states $P_c^+(4450)$ with spin 3/2 and 5/2, corresponding to the resonance energy. Notice that the curves labeled t-channel are expected to be the main

background in the observation of the P_c^+ states. As it is shown in the following, compared to the polarization observables K_{LL} and A_{LL}, the differential cross-section is less capable of differentiating the different photo-couplings contributions.

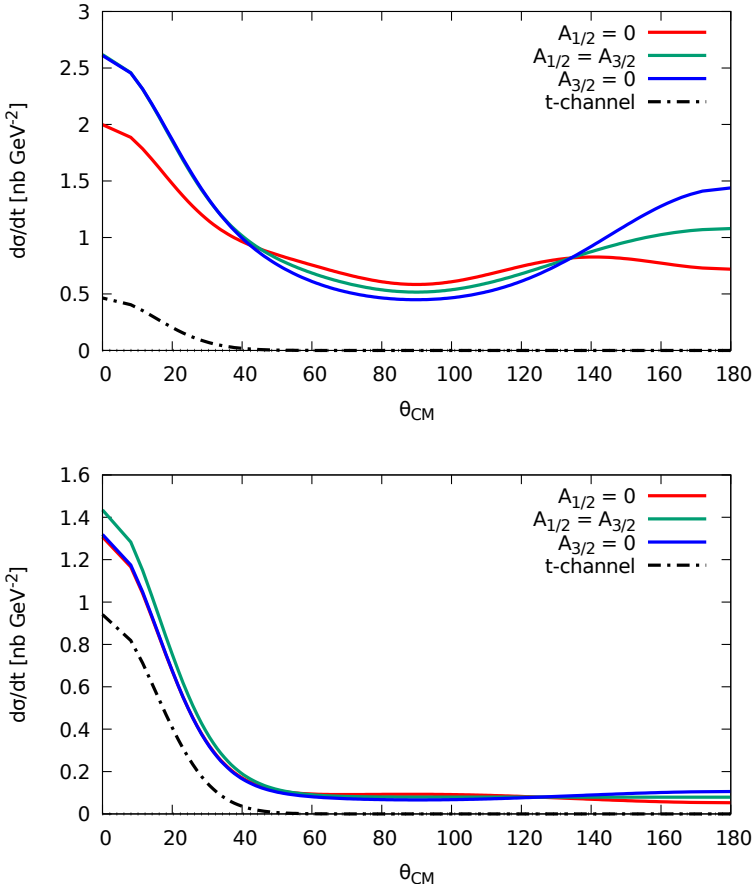

Figure 4: The CM angular dependence of $P_c^+(4450)$ photoproduction differential cross-section for three different scenarios of the photo-couplings at the resonant energy: (top) the spin $\frac{5}{2}^+$ state case, and (bottom) the $\frac{3}{2}^-$ one, both with branching fraction of 2%.

Fig. 5 shows the predictions of both K_{LL} and A_{LL} in the forward direction for all the possible spin-parity assignments, assuming equal photo-couplings: (top) corresponds to the $P_c^+(4450)$ $5/2^+$ separately and (bottom) to both $P_c^+(4450)$ $5/2^+$ and $P_c^+(4380)$ $3/2^-$. At forward angle there is a large distinguishing power of the different spin-parity states of the pentaquarks. The t-channel background provides values of the polarization observables close to zero.

- Fig. 6 shows the predictions for A_{LL} and K_{LL} for $P_c^+(4450)$ $5/2^+$ and $P_c^+(4380)$ $3/2^-$ at a scattering angle of the reaction in the center of mass of 45 degrees, for different values of the photo-couplings. The (top) figure shows the contribution from the narrow state only,

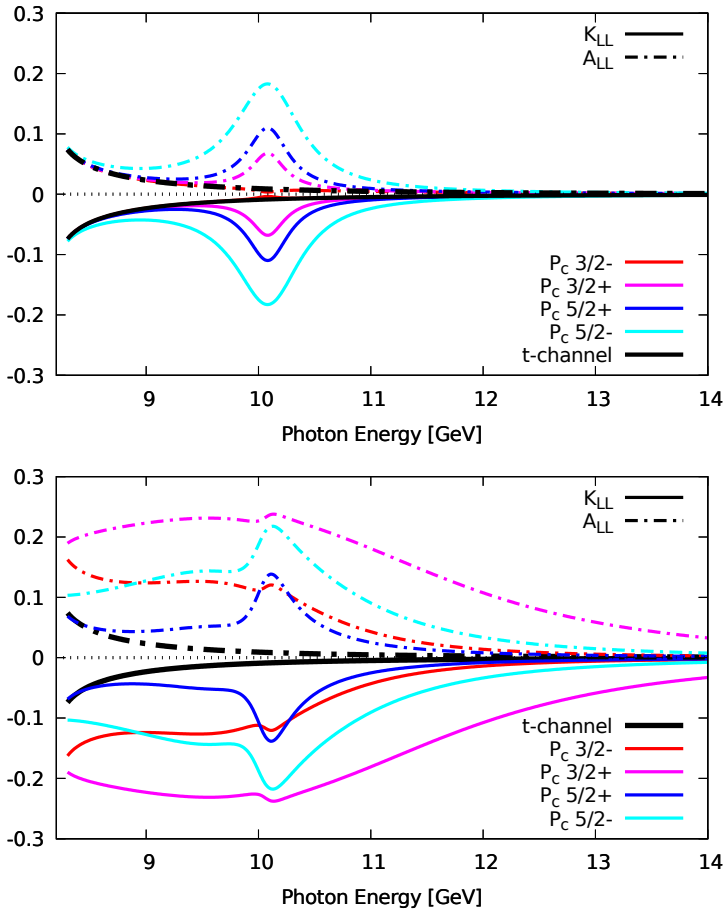

Figure 5: (top) Predictions for K_{LL} and A_{LL} as a function of the energy for all the possible quantum numbers assignment of the $Pc^+(4450)$. (bottom) The same predictions adding the contribution from the wider $P_c^+(4380)$ with spin-parity $3/2^-$. These plots correspond to the forward direction in the center of mass and assume equal photo-couplings.

whereas the lower is by adding both pentaquarks. A general consideration is that at this angle, for equal photo-couplings the distinguishing power between t-channel and resonance contribution is reduced compared to the forward case. Nevertheless, with the quantum numbers and branching fractions chosen in these plots, there is high sensitivity to the photo-couplings (especially for A_{LL}), which can be clearly distinguished in the extreme case where one of the two couplings is zero. We point out that the choice of the quantum numbers and branching ratio is arbitrary and that different scenarios are possible to which A_{LL} and K_{LL} can be sensitive.

As it is clear from Figs. (5,6) there is a peak structure corresponding to the resonance energy for the state $P_c^+(4450)$, whose intensity depends on its quantum numbers and couplings. The observation of such a peak at the resonance energy would represent a clear signature of a P_c^+ state. Such a state should be observable in both A_{LL} and K_{LL}. The distinguishing

power in the two observables can be different and vary with the features described above.

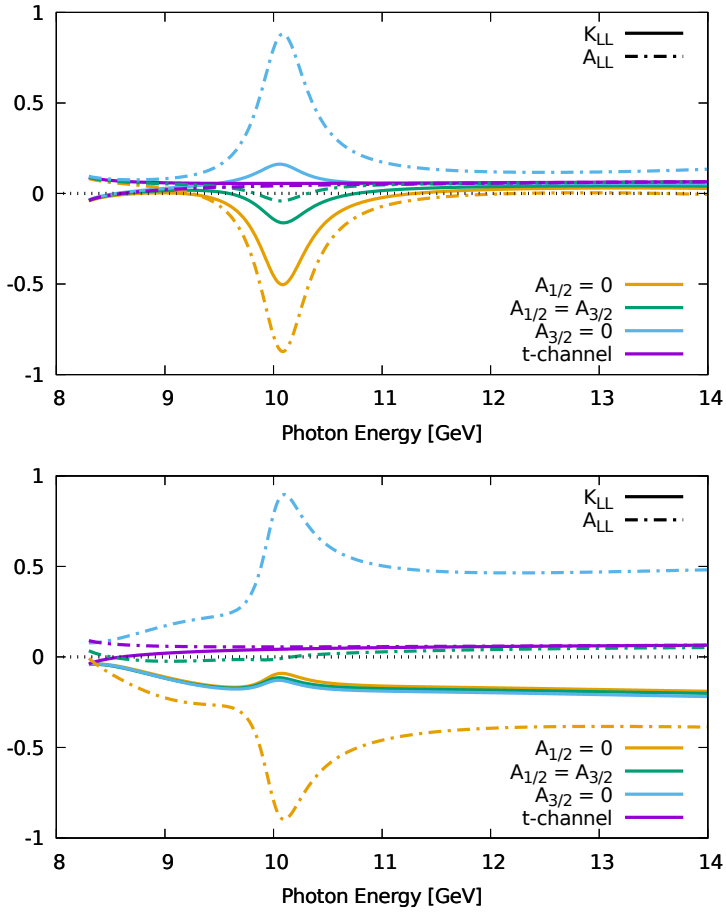

Figure 6: The A_{LL} and K_{LL}predictions at 45° in the CM for $P_c^+(4450)$ with spin-parity $5/2^+$ and $P_c^+(4380)$ with $3/2^-$, for different values of the photocouplings assuming 2% branching ratio in the hadronic decay of the pentaquarks. (top) shows the $P_c^+(4450)$ contribution only, whereas (bottom) combines the two states.

3 Experimental Aspects

This experiment is designed to study the exclusive process $\gamma p \to P_c \to J/\psi(e^+e^-) + p'$ by measuring the polarization observables A_{LL} and K_{LL}. The experimental apparatus presented in this section allows to reach a high (close to 0.65%) acceptance for the events with all three final state particles to be detected.

For the K_{LL} measurement, an electron beam of 5 μA will pass through a 6%X0 Cu radiator and then (together with the photons produced in the radiator) interacts with a 15-cm long liquid hydrogen target. A polarimeter will be used in the proton arm to measure the azimuthal asymmetry in direction of the proton after scattering in the CH2 analyzer.

For the A_{LL} measurement, a NH3 polarized target with polarization direction along the beam direction will be used with an electron beam of 100 nA and a 10%X0 Cu radiator located upstream of the target.

The photon-proton luminosity of 1.7×10^{36} of equivalent photon/s - unbounded target protons/cm^2 for the K_{LL} measurement and one hundred times lower for A_{LL}. The K_{LL} luminosity is resulting in rate of 130 Hz $J/\psi + p$ produced and 7.8 Hz $J/\psi + p$ with e^+e^- pair. The detected event rate will be 0.051 Hz or 4400 per day (assuming the resonance parameters 2% branching to J/ψ+ proton (5 nb production cross section) and 40 MeV width of the resonance). The lower luminosity for A_{LL} is compensated by a higher figure-of-merit in the experiment with a polarized target.

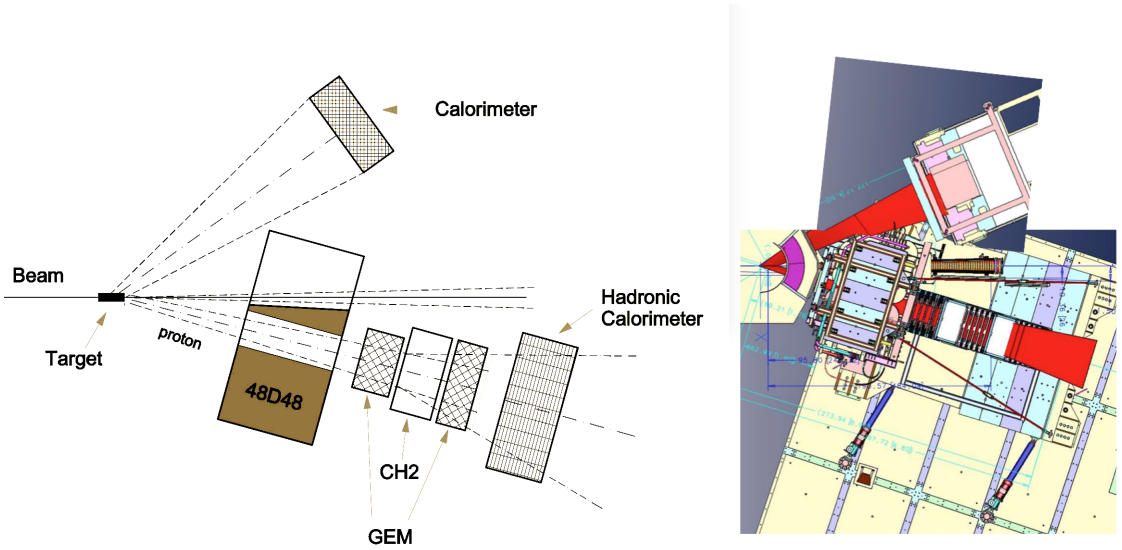

Figure 7: Sketch of the experiment for the measurement of the polarization observables in SBS. The detailed layout on right is based on SBS/ECAL configuration for Q^2=12 GeV^2 run for GEp experiment but relocation of ECAL to 5.5 degrees smaller angle. For the A_{LL} measurement, the polarized target will be used with polarization along the beam direction. For the K_{LL} measurement, a polarimeter will be used in the proton arm to measure the azimuthal asymmetry in direction of the proton after scattering in the CH2 analyzer.

Experimental setup consists of two arms that we will call "hadronic arm" and "electron arm". However, note that for this experiment the hadronic arm will register in addition one of the leptons from the J/ψ decay. There are three topologies that could be considered for three particles in two arms: (i) p, e^+ in SBS and e^- in ECAL, (ii) p, e^- in SBS and e^+ in ECAL, and (iii) p in SBS and e^+, e^- in ECAL. The topologies (i) and (ii) with two particles reconstructed in SBS are preferred due to better resolutions on the invariant mass of J/ψ and on the reconstructed incident energy, see Tab. 1.

Table 1: The preferred topologies in the reconstruction of exclusive (with a recoil proton) J/ψ events. Details on the resolution studies can be found in Sec. 4.5.

topology	SBS	ECAL	resolution on M and E
(i)	p, e^+	e^-	✔
(ii)	p, e^-	e^+	✔
(iii)	p	e^+e^-	✗

The hadronic arm is a large acceptance magnetic spectrometer combined with a polarimeter and a hadronic calorimeter for particle energy measurement (see Sec. 3.1 for details). The SBS magnet is placed at 17 degrees (a central angle) followed by a wide area GEM tracker, a CH_2 analyzer (for the K_{LL} measurement), another GEM tracker, and hadron calorimeter (HCAL). A total range of horizontal angle for SBS is from 12.9 to 21.3 degrees. The field in the SBS magnet is adjusted to match momentum range of the protons (lowest momentum is just 1 GeV/c). For K_{LL} measurement projected result we took into account the spin precession angle in the SBS magnet.

The electron arm, with central angle at about 22 degrees in respect to the beam direction, consists of a highly segmented electromagnetic calorimeter (see Sec. 3.2 on ECAL) and a scintillator coordinate detector in front (as in the GEp experiment). Installation of both arms at small angle is possible because for required magnetic field in SBS the small angle coils of the magnet will not be used.

For the measurement of the polarization transfer K_{LL}, we propose to use a circularly polarized photon beam created from an incident polarized electron beam of 5 μA by bremsstrahlung on 6% Cu radiator and a 15-cm long liquid hydrogen target. The choice of the beam intensity leads to comfortable rate of background in the tracker detector of SBS and trigger. Alternatively, experiment can use 20 μA electron beam without the radiator and a bit higher rate of high energy electrons in the detectors. The measurement of A_{LL} differs from K_{LL} in that a polarized target NH_3 will be used. With these beam parameters effective photon intensity could be also expressed as $0.7{\cdot}10^{11}$ equivalent gamma per second. The photon flux could be enhanced by a factor of 30 if the experiment will use a Compact Photon Source. However, even without such potential gain the projected accuracy of A_{LL} is the same as for K_{LL}parts.

The logic of trigger for the data collection system is based of the total energy detected in two calorimeters (ECAL and HCAL). ECAL calorimeter signal should be above 3.5 GeV, HCAL signal should be above 2.5 GeV, and the combined signal above 7 GeV. These high

threshold conditions will lead to acceptable counting rate of the trigger on the level of 2.5 kHz. The data flux will be about ten times lower than in GEp/SBS experiment due to the lower luminosity in this proposal which results in modest occupancy in the GEM tracker.

Table 2: The projected electron beam intensity, radiator thickness, photon flux in the units of equivalent photon/s, the free proton-photon luminosity, and the total luminosity for the K_{LL} and A_{LL} measurements.

	I_e [μA]	radiator, X0	I_γ [γ/s]	$\rho_{free\ \ protons} \cdot l$ [g/cm^2]	$\mathcal{L}_{free\ \ proton}$ [cm^{-2}s^{-1}]	$\mathcal{L}_{total}$ [cm^{-2}s^{-1}]
K_{LL}	5.0	6%	$2.6 \cdot 10^{12}$	1.08	$1.7 \cdot 10^{36}$	$1.8 \cdot 10^{36}$
A_{LL}	0.1	10%	$0.7 \cdot 10^{11}$	0.32	$1.3 \cdot 10^{34}$	$4.0 \cdot 10^{34}$

The expected resolutions for the SBS and ECAL are shown in Tab. 3. The table contains also the main parameters of the experimental setup configuration.

Table 3: The geometry and resolutions for SBS (at reduced magnetic field) and ECAL.

SBS, p and e^+/e^-		ECAL (e^- or e^+)	
Angle	17.0°	Angle	22.0°
Distance	385 cm (to the last chamber of FT)	Distance	400 cm
$\sigma(P)/P$ (%)	0.73 + 0.075 · p [GeV/c]	$\sigma(P)/P$ (%)	$9/\sqrt{E[GeV]}$

3.1 The SBS proton arm

In this experiment the SBS [24] is configured to detect the recoil proton along with one of the two leptons from the J/ψ decay. The SBS (hadronic arm) includes a magnet placed at 17 degrees followed by a GEM front tracker (FT), a (60×200 cm^2) CH_2 analyzer (for the K_{LL} measurement), a second GEM tracker (100×200 cm^2) (ST), and a hadron calorimeter (HCAL). An important consideration in the design of the hadronic arm is related to the polarization transfer measurement. Given the low average momentum of the scattered proton, about 1-2 GeV/c, to maximize the analyzing power one has to put the HCAL a bit closer to the analyzer than it is for GEp experiment. The GEM modules for FT are designed and fabricated by INFN-Roma and INFN-Catania. The GEM modules for ST are designed and fabricated by UVa group [25]. The proton polarimetry technique allows to measure the polarization transfer in the longitudinal and transverse direction with respect to the recoil proton momentum. The elastic e-p scattering will be used to calibrate the polarimeter for the proton momentum of this experiment.

The HCAL for SBS is mainly designed to detect the recoiling protons or neutrons. HCAL has modular structure with 288 blocks arranged in a matrix 12×24. It provides a spacial resolution of 4-5 cm and energy resolution for proton of 60% for 1 GeV proton. However, HCAL also can be used for measurement of the electron(positron) energy. The energy resolution of HCAL for an electron is about $14\%/\sqrt{(E[GeV])}$.

3.2 The ECAL arm

The electromagnetic calorimeter ECAL is designed to have a C-shape according to the phase-space kinematics of the scattered electron from elastic scattering $ep \to e'p'$. Lead-glass crystall is attached to the light guide in ECAL. Each 'super-module' is designed to contain 9 lead-glass scintillators and the support attachment of 9 boron silicate glass light guides connected to photomultiplier tube bases. The expected resolution on shower energy is $9\%/\sqrt{\mathrm{E[GeV]}}$. The coordinate resolution of 0.5 cm will be from ECAL itself. The vertical resolution will be improved to 0.2 cm by means of the Coordinate detector. The corresponding angular resolution is 1.2 and 0.5 milli radian for proposed location of ECAL. The width and height of the support structure are about 120×300 cm^2. A schematic representation of the calorimeter can be seen in Fig. 8.

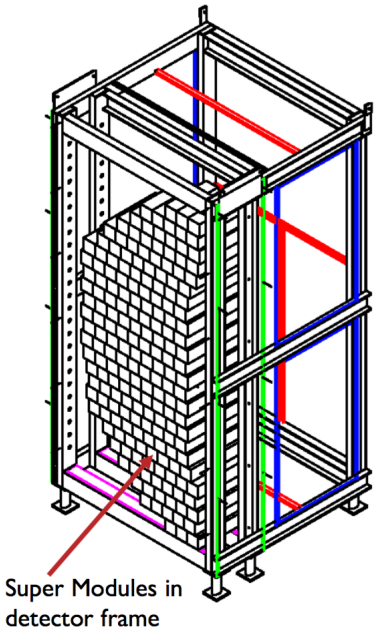

Figure 8: Picture is taken from Ref. [26]

4 Simulation of the Experiment

4.1 Event Generator

We simulated both, the s-channel pentaquark production, $\gamma p \to P_c \to J/\psi + p'$ and the t-channel $\gamma p \to J/\psi + p'$. (see Fig. 2): The event generator used to study the background t-channel and the resonance is based on the JPAC model for both processes [27]. A slope of 1.2 GeV^2 is used for the t-channel reaction. A spin/parity of $5/2^+$ for $P_c(4450)$ and $3/2^-$ for $P_c(4380)$, the preferred choice of the LHCb experiment, is used in modeling the resonance.

The J/ψ takes most of the energy available in the reaction and in lab frame, it is produced forward at a small angle. The distributions of the proton lab angle as a function of the four momentum transfer, t, and the proton momentum are shown in Fig. 9 for different beam energies. We maximize the acceptance in the $\sim$ 10 GeV region, where we expect the peaks of the pentaquarks, therefore the proton angle should be around 20°. Since one of the leptons is registered in the proton arm, the other lepton goes at a slightly bigger angle in the electron arm.

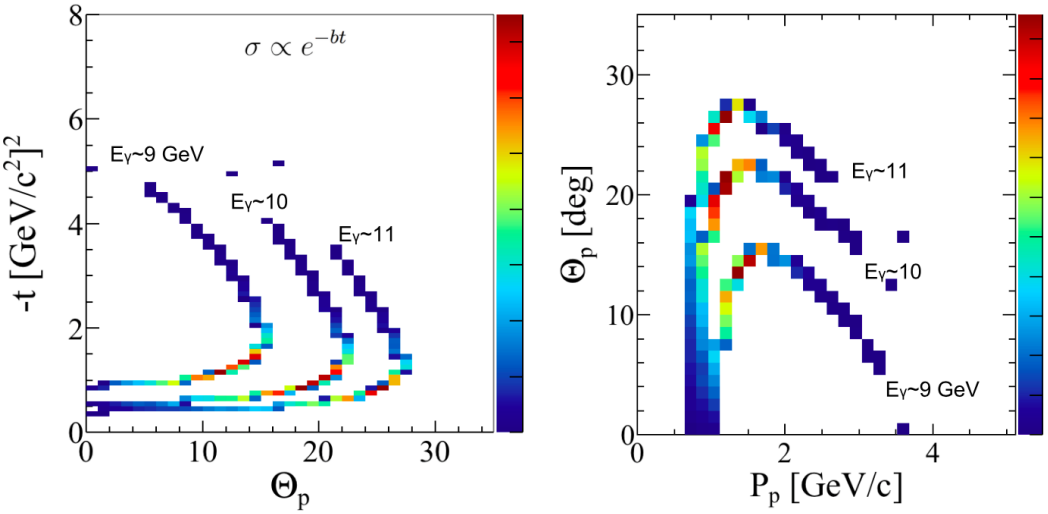

Figure 9: The kinematics of the t-channel J/ψ: (left) The momentum transfer $-t$ as a function of the proton polar angle in the lab plane in bins of the photon beam energy; (right) The distribution of the proton angle vs the proton momentum. The thrown distributions are scaled to arbitrary units.

4.2 Physics Background

The largest background to the pentaquark states $P_c^+(4380)$ and $P_c^+(4450)$ is the t-channel exclusive photo-production of $\gamma p \to J/\psi + p'$ discussed in the previous section. Another background is the Bethe-Heitler (BH) processes , whose diagram is represented in Fig. 10.

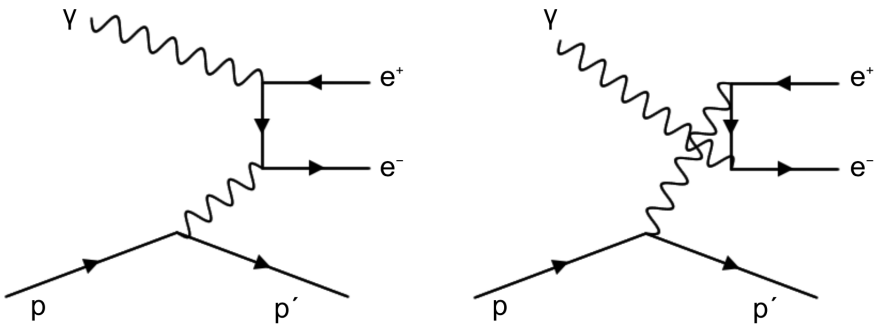

Figure 10: Bethe-Heitler process diagrams

This is an electro-magnetic process and, with a high confidence, is expected to be 10 times smaller than the t-channel background as estimated in the Hall C proposal [15].

Another physics background considered in the Hall C proposal is associated with the inelastic channel of the J/ψ production, where an additional final state pion is produced but not registered in the detectors: the cross-section was found to be less than 30% of the corresponding elastic t-channel cross-section at high energy, and the dominant contribution in this region is the resonant channel $\gamma p \to J/\psi\Delta$ with a threshold above 9 GeV. In contrast to the Hall C experiment, we register all the three final state particle which allows to estimate the missing mass with a resolution significantly exceeding the mass of the pion, thus excluding this reaction. Finally another source of background can arise from lepto-production events $ep \to eJ/\psi p$, with an expected impact only from those events characterized by quasi-real photons given that photons with higher virtuality are highly suppressed. The effect of the electro-production contribution is that of causing a small enhancement in the count rates. Therefore, in this paper we consider the t-channel production as the main physics background, while all the other processes are an order of magnitude smaller.

4.3 Accidental coincidence rate

The single background rates for p, $e^{\pm}$, $\pi^{\pm}$ in the two arms have been estimated using the results from the CHIPS model [28] and empirical data from WACS 99-114 experiment. Results for 1 GeV threshold in both arms are shown in Table 4.

The trigger will use 2.5 GeV threshold for the HCAL in SBS and 3.5 GeV for ECAL. Based on the simulated performance of the calorimeters we expect the rates to be 8 and 84 times lower, respectively for HCAL and ECAL, than the rates for 1 GeV shown in the table. The distributions of the particles in the detector acceptance for events where the topology is fully reconstructed are shown in Fig. 11. Assuming a 50 ns trigger window between the two arms, the accidental coincidence rate was found to be of the order of 2.5 kHz.

SBS Θ_c=17°			ECAL Θ_c=22°	
e(Hz)	π(Hz)	p(Hz)	e(Hz)	π(Hz)
2.5×10^4	3×10^6	4×10^5	4×10^5	8×10^6

Table 4: Estimates of the single background rates. Thresholds 1 GeV/c have been assumed for both, HCAL in SBS and ECAL..

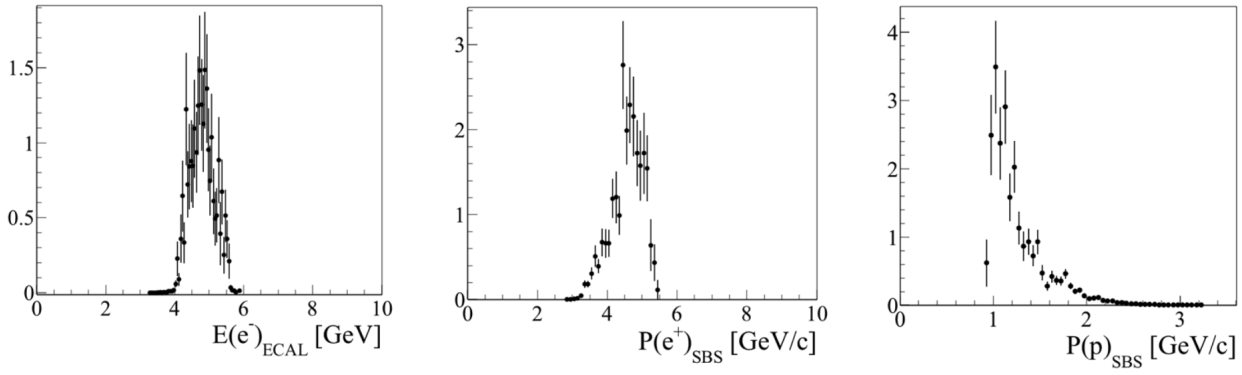

Figure 11: Distributions of (left) electrons energy reconstructed in ECAL, (center) positron and (right) proton momenta reconstructed in SBS.

4.4 Acceptance Studies

A sketch of the experimental setup for the SBS and ECAL arms is shown in Fig. 7. The experiment has been designed to maximize the geometrical acceptance in the 10 GeV photon energy region. The optimization has been done using a toy Monte Carlo model that uses as an input the event generator as described above. The model includes transport through the magnet, as well as simulations of the polarimeter as described later. The sensitive areas of the detectors are used to define the acceptance of the experiment.

The acceptance has been considered as a 'black-box' function of different parameters (i.e. the central angles of ECAL and SBS, the distance from the target center and the width of ECAL) with some mechanical and engineering constraints and detector configuration as described in Sec. 3. Table 5 summarizes the main beam parameters and the detector configuration (same for both A_{LL} and K_{LL} measurements), as well as acceptances which include both topologies (i) and (ii) defined in Tab. 1.

4.5 Resolution Studies

The advantage of using topology (i) and (ii) is that the beam energy can be determined directly from the momenta of the particles measured in SBS arm, with resolution reported

Table 5: Kinematics and main parameters of the A_{LL} and K_{LL} experiments running at E_e= 11 (GeV). The final column reports the geometrical acceptance. Distances are from target: d_{SBS} corresponds to the location of the most distant tracking chamber, whereas d_{ECAL} corresponds to ECAL. The sensitive area of $3m^2$ of ECAL is rearranged over a width of about 1.2 m.

				SBS			ECAL		
experiment	I_e (μA)	R.L. (%)	L_{target} (cm)	Θ_c (deg)	d (cm)	$\int B \cdot dl$ [T·m]	Θ_c (deg)	d (cm)	A (%)
K_{LL}	5.0	6	15	17	485	1	22	400	0.65
A_{LL}	0.1	10	3	17	385	1	22	400	0.65

in Tab. 3, according to Eq. (6):

$$\begin{aligned} E^p_{beam} &= \frac{a^2 - p_T^2 - p_L^2}{2(a - p_L)} \\ M_{J/\psi} &= \sqrt{2 \cdot \left[E^p_{beam} M_p + M_p^2 - (E^p_{beam} + M_p) E_p + E^p_{beam} p_p \cos\theta_p\right]} \end{aligned} \tag{6}$$

where

$$\begin{aligned} a &= E_p + p_{e^+} - M_p \\ p_T^2 &= (p_p + p_{e^+})_T^2 \\ p_L &= (p_p + p_{e^+})_L \end{aligned} \tag{7}$$

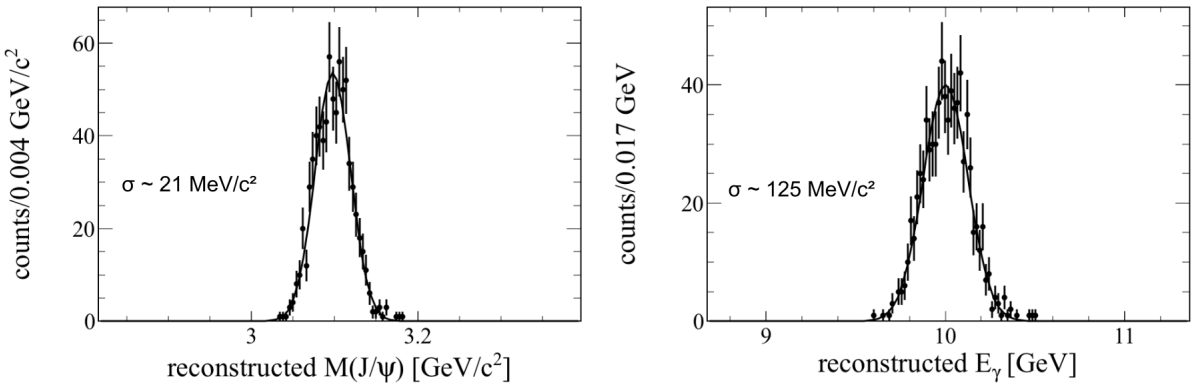

Figure 12: (left) Reconstruction of J/ψ invariant mass and (right) the incident photon energy by Eq. (6). Both distributions have been obtained using the reconstructed proton and a lepton measured in SBS according to combining the topologies (i) and (ii), that is p,$e^{\pm}$ detected in SBS (and $e^{\mp}$ tagged in ECAL). The MC sample corresponds to a nominal photon beam energy of 10 GeV.

The reconstructed mass and beam energy off the SBS arm based on Eq. (6) and their corresponding resolutions are shown in Fig. 12 top left and right, respectively. The per-particle resolutions used in this simulation have been taken from Tab. 3. We can improve

further the resolutions by using in addition the angle and energy of the lepton registered in ECAL using a kinematic fit, which however has not been done in this LoI.

4.6 Event Selection

As previously discussed the signal candidate events are characterized by the reconstruction of the proton and one lepton in the SBS arm, with the other lepton detected in ECAL. The main cuts are aimed to suppress the pion background.

For the lepton in the SBS arm, we apply E/p cut, where the energy is measured in HCAL and momentum in the spectrometer. The simulated relative resolution for electrons in HCAL is $14\%/\sqrt{E}$. The E/p cut for the lepton in ECAL uses the energy from the calorimeter ($9\%/\sqrt{E}$ resolution) and the momentum predicted from the measured momenta of the other two particles and the reconstructed beam energy. The pion rejection power in the hadron calorimeter is much lower since both pions and electrons with a given energy will peak at the same position, just pions have wider distribution. Therefore, if needed, we consider installing a pre-shower detector in front of HCAL. Further rejection of the background will be achieved by constraining the production vertex from the two tracks measured in SBS. Finally, we apply cuts around the reconstructed J/ψ mass.

4.7 Polarimetry for $\mathbf{K_{LL}}$ measurements

This experiment benefits from the fact that the proton-nucleus analyzing power increases significantly at low proton momenta of 1-2 GeV, with an average $< p >= 1.2$ GeV (see Fig. 11). Measurements of the analyzing power in this momentum range on Carbon have been done in [29]. The Figure of Merit defined as, $F = A_y * \sqrt{\epsilon_{pol}}$, where A_y is the analyzing power and ϵ_{pol} is the polarimeter efficiency, averaged over $4 - 18^\circ$, is shown in Fig. 13. Note that labels in the figure correspond to proton *kinetic* energy. For the proposed experiment we will use 30cm CH_2 analyzer; it is know that this material compared to Carbon, has a slightly better analyzing power. Using the parametrizations from [29], our simulations result in average Figure of Merit squared of $< F^2 >= 0.014$. The longitudinal spin of the proton rotates in the magnet to an average precession angle of $\chi_{prec} = 42^\circ$ and the polarimeter measures only the *transverse* component of the proton spin. Therefore, we define the effective Figure of merit as $F_{eff} = F sin(\chi_{prec})$, for which we obtain from the simulations an average of $< F_{eff} >= 0.072$, which value enters in the $\mathrm{K_{LL}}$ error estimate.

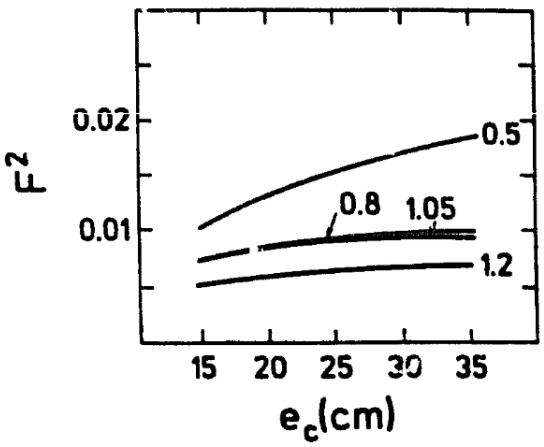

Figure 13: The Figure of Merit squared from [29] as a function of the Carbon analyzer thickness in cm, for different proton kinetic energies in GeV as labeled.

5 Projected Results

The event rates of the process $\gamma p \to J/\psi + p'$ are the products of the luminosity, the cross section, the acceptances of the detectors, as well as the branching fraction of the channel in which J/ψ decay, namely BR($J/\psi \to e^+e^-$) = $B_{e\pm}$ = 5.94%. The projected number of events per day was estimated as:

$$N_{J/\psi+p}/\text{day} \approx \int_{E_{res}-\Delta E_\gamma/2}^{E_{res}+\Delta E_\gamma/2} N_\gamma \cdot \frac{dE_\gamma}{E_\gamma} \cdot \underset{(\text{p/cm}^2)}{t} \cdot \underset{(5\ nb\ at\ res.)}{\sigma(E_\gamma)} \cdot \underset{(0.65\%)}{\epsilon} \cdot \underset{(5.94\%)}{B_{e\pm}} \cdot \underset{(80k\ s)}{\text{time}} \qquad (8)$$

In Eq. (8), σ is the photo-production cross-section (e.g. of $\gamma p \to P_c \to J/\psi + p'$) as a function of the incident photon energy, N_γ is the equivalent photon flux, E_{res} is the resonance peak position in the photo-production spectrum, ΔE_γ is the photon energy range of interest, t is a product of the target density for unbounded protons and length, ϵ is the detection acceptance.

It is interesting to compare at the resonance energy the rates of the resonant contribution $\gamma p \to P_c \to J/\psi + p'$ (under certain spin-parity and couplings assumption) to that corresponding to the t-channel production $\gamma p \to J/\psi + p'$. The resonance energy is determined through the amplitude $< \lambda_{J/\psi}\lambda_{p'}|T_{res}|\lambda_\gamma\lambda_p > \sim \frac{1}{M_{res}^2 - s}$, where λ are helicity states of the particles in the initial and final states. Therefore, the energy corresponding to the mass of the narrowest of the two LHCb pentaquarks, namely M_{res}= 4450 MeV/c^2, is $E_{res} \sim 10.1$ GeV. With the experimental setup, we expect to record about 4400 exclusive (with the recoil proton) J/ψ events per day, assuming 2% branching of pentaquark decay to J/ψ + p.

Based on the simulated events described above, we can calculate the statistical uncertainty on $A_{LL}$and K_{LL}according to:

$$\Delta A_{LL} = \frac{2}{\sqrt{\frac{N_{P_c^+}}{D}} \cdot P_p \cdot P_\gamma} \qquad (9)$$

and

$$\Delta K_{LL} = \frac{2}{\sqrt{\frac{N_{P_c^+}}{D}} \cdot < \sqrt{\epsilon_{polarimeter}} A_y \sin\chi_{prec} > \cdot P_\gamma} \qquad (10)$$

where $N_{P_c^+}$ is the total number of pentaquark candidates from exclusive J/ψ events accumulated with a polarized target or with the polarization transfer experimental setup, while D is the background dilution factor (whose value is close to one). P_γ = 0.70 is the photon beam polarization, P_p = 0.75 is the average proton polarization at target, $\epsilon_{polarimeter}$ is efficiency of the polarimeter, A_y is the polarimeter analyzing power, and χ_{prec} is the spin precession angle in the SBS magnet.

A projection of the uncertainty on the A_{LL} measurement with 20 days of beam is shown in Fig. 14.

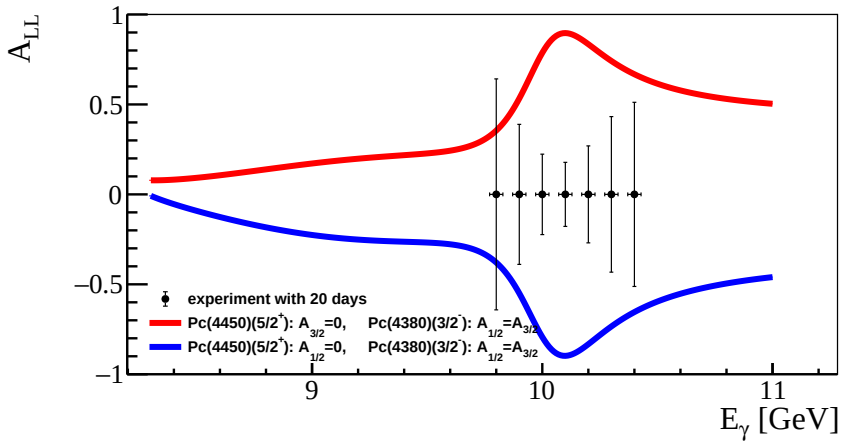

Figure 14: Projected uncertainty on A_{LL} with 20 days of beam. The predictions are at a center of mass angle of θ_{cm} =45°. They include both the wide $P_c^+(4380)$ $3/2^-$ and narrow $P_c^+(4450)$ $5/2^+$ states. The hadronic branching ratio of both P_c^+ are fixed at 2%. Scenarios can change significantly by varying the BRs. Notice that the photo-couplings of both P_c^+ are varied, as specified in the legend, and different combinations are shown.

6 Summary

This proposal is focused on determining the polarization observables characterizing the reaction $\gamma p \to P_c \to J/\psi + p'$ with the goal to confirm the LHCb observations as well as to investigate the strengths of the pentaquark couplings in the initial and final state, the determination of which is a non-trivial issue, and high sensitivity is just of paramount importance. Recent calculations developed in collaboration with JPAC proved that the polarization observables are sensitive to both the photo-coupling and the hadronic coupling of the pentaquarks, and therefore their determination would allow to get a comprehensive picture of these new P_c^+ states.

An experimental setup for SBS reused from the GEp experiment is proposed to measure for the first time the helicity correlation distributions between the incident photon and the proton at target (A_{LL}) as well as the polarization transferred from the incident photon to the recoil proton (K_{LL}), for exclusively photo-produced $J/\psi+$ p events.

The key of any search is the rate of events and sensitivity of the observables to parameters of the pentaquark states. We expect to have 4400 events per day from the 4.45 GeV resonance assuming 2% branching ratio to $J/\psi+$ p.

These measurements will help shed light on the mechanism underlying the photo-production of J/ψ in the t-channel and will provide at the same time a new independent source of information on the pentaquark spin-parity in addition to cross-section measurements performed in other experiments at Jefferson Lab. Remarkably, the polarization observables show an excellent sensitivity to both photo-couplings and hadronic coupling, respectively related to the production and decay mechanisms of the pentaquark, and their study and characterization can open new unprecedented scenarios.

References

[1] M. Gell-Mann, Phys. Lett. **3** (1964), no. 8 214,215.

[2] T. Nakano *et al.*, Phys. Rev. Lett. **91** (2003), no. 1 012002.

[3] C. Alt *et al.*, Phys. Rev. Lett. **92** (2004), no. 4 042003.

[4] A. Aktas *et al.*, Phys. Lett. B **588** (2004), no. 1-2 17.

[5] B. McKinnon *et al.*, Phys. Rev. Lett. **96** (2006), no. 21 212001.

[6] V. Barmin *et al.*, Phys. Rev. C **89** (2014), no. 4 045204.

[7] J. Barth *et al.*, Phys. Lett. B **572** (2003), no. 3-4 127.

[8] R. Aaij *et al.*, Phys. Rev. Lett. **115** (2015), no. 7 072001.

[9] L. Maiani, A. Polosa, and V. Riquer, Phys. Lett. B **749** (2015) 289.

[10] R. Chen, X. Liu, X.-Q. Li, and S.-L. Zhu, Phys. Rev. Lett. **115** (2015), no. 13 132002.

[11] F.-K. Guo *et al.*, Phys. Rev. D **92** (2015), no. 7 071502.

[12] A. Austregesilo *et al.*, arXiv:1801. 05332 (2018).

[13] The Hall B Collaboration, *E12-12-001A, proposal to JLab-PAC45*, 2017.

[14] The ATHENNA Collaboration, *PR12-12-006, proposal to JLab-PAC39*, 2012.

[15] Z.-E. Meziani *et al.*, arXiv:1609. 00676 (2016).

[16] The Hall A Collaboration, *PR12-07-109*, 2007.

[17] `https://www.jlab.org/exp_prog/PACpage/PAC32/PAC32_report.pdf`, 2007.

[18] B. Wojtsekhowski, *SBS project overview and status, SBS collaboration meeting*, 2017.

[19] C. Fanelli, L. Pentchev, and B. Wojtsekhowski, Bulletin of the APS (2018).

[20] D. Winney, A. H. Blin, A. Pilloni, A. Szczepaniak, et al. (JPAC Coll.), *to appear*, 2018.

[21] Hiller Blin and others (JPAC Coll.), Phys. Rev. **D94** (2016) 034002.

[22] F. E. Close and G. A. Schuler, Phys. Lett. **B458** (1999) 127.

[23] Karliner, Marek and Rosner, Jonathan L. , Phys. Lett. **B752** (2016) 329.

[24] The Hall A Collaboration, *The SBS for Jefferson Lab Hall A (CDR)*, 2009.

[25] K. Gnanvo, N. Liyanage, V. Nelyubin, K. Saenboonruang, S. Sacher, and B. Wojtsekhowski, Nucl. Instrum. Methods Phys. Res. **782** (2015) 77.

[26] C. R. Jackson, *The SBS Electromagnetic Calorimeter (ECAL) Development*, 2017.

[27] Joint Physics Analysis Center, Jefferson Lab, *Simulation code for* $\gamma p \to J/\psi + p'$, 2018.

[28] P. Degtyarenko, M. Kossov, and H.-P. Wellisch, Eur. Phys. J. A **3** (2000), no. 8, 217.

[29] B. Bonin et al., NIM **A288** p.379 (1990). .